AIP Journal of Applied Physics

Magnetic force microscopy investigation of domain structures in Fe – x at. % Ga single crystals (12 x 25)

Feiming Bai, Jiefang Li, D. Viehland, D. Wu, and T. A. Lograsso

Citation: Journal of Applied Physics **98**, 023904 (2005); doi: 10.1063/1.1978971
View online: http://dx.doi.org/10.1063/1.1978971
View Table of Contents: http://scitation.aip.org/content/aip/journal/jap/98/2?ver=pdfcov
Published by the AIP Publishing

Magnetic force microscopy investigation of domain structures in Fe–*x* at. % Ga single crystals (12<*x*<25)

Feiming Bai,[a] Jiefang Li, and D. Viehland
Department of Materials Science and Engineering, Virginia Tech, Blacksburg, Virginia 24061

D. Wu and T. A. Lograsso
Metals and Ceramics, Ames Laboratory, Ames, Iowa 50011

(Received 13 January 2005; accepted 20 May 2005; published online 21 July 2005)

The domain structure of furnace-cooled (FC) and post-annealed (PA) Fe–*x* at. % Ga (*x*=12, 20, and 25) crystals has been investigated by magnetic force microscopy. For both FC and PA Fe–12 at. % Ga, the domains were found to be well-aligned and oriented along the [100] direction. For Fe–20 at. % Ga, although a preferred [100] orientation remained, a difference in morphology was found between FC and PA conditions—in the PA condition, clear dendritic domains were observed. For both FC and PA Fe–25 at. % Ga, a much reduced [100] preferred domain orientation was found, the domain size was notably reduced, and dendrite formation was not observed. © *2005 American Institute of Physics*. [DOI: 10.1063/1.1978971]

I. INTRODUCTION

Magnetostrictive materials are widely used in various sensor and actuator applications.[1] Recently, Clark *et al.*[2] found a large magnetostrictive strain of $\lambda_{100}>200$ ppm at room temperature in Fe–Ga bcc single crystals, which is $\sim 10\times$ that of pure Fe. This result demonstrates that the magnetostriction of Fe can be dramatically enhanced by the substitution of nonmagnetic elements. A similar finding was previously reported by Hall,[3] who found that the addition of Al to Fe enhanced λ_{100} by $\sim 4\times$. Also, a magnetostriction of about −700 ppm has been reported in melt-spun $Fe_{81}Al_{19}$ that is $\sim 5\times$ that of corresponding bulk materials,[4] and a value of $\lambda_{100}\sim 1100$ ppm has been found in melt-spun stacked Fe–15 at. % Ga ribbons.[5] Finally, Fe–Ga alloys have additional advantages[6] over commercially available magnetostrictive Terfenol-D such as (i) high mechanical strength, (ii) good ductility, and (iii) high imposed stresses, which are particularly good at low applied magnetic fields ($H<150$ Oe).

The solubility of Ga in α-Fe is known to be large—up to 36 at. % at 1037 °C. Thus, compositions within the Fe–Ga solution can be made with quite high Ga contents. This has important ramifications to the magnetostriction properties near room temperature. As shown in Fig. 1, the value of λ_{100} first increases with increasing Ga content, reaches a maximum for $x\sim 17-19$, and subsequently sharply decreases with further increment in x, but exhibits a second peak near $x\sim 27$. Furthermore, these trends are dependent upon the thermal history of the Fe–Ga crystal.[7] In the furnace-cooled (FC) condition, the maximum in λ_{100} is reached at $x=17$; whereas in the rapidly quenched (RQ) condition, the value of λ_{100} continues to increase with increasing Ga content until $x=19$. Structural studies[8] have shown that the thermal history dependence of the magnetostriction in the vicinity of $17<x<19$ is due to the stabilization of the disordered bcc structure (i.e., the A2 phase) by quenching. However, for $x>20$, where the magnetostriction dramatically decreases with increasing x, the dominant phase was found to be the long-range-ordered B2 or DO3 structure. Furthermore, with increased quenching rate, the disordered bcc structure can be stabilized to even higher concentrations of nonmagnetic substituents (Al or Ga).

However, to date, investigations of the magnetic domain structure of Fe–*x* at. % Ga crystals have not been reported. Such studies could provide important information concerning the origins of the enhanced magnetostriction and why the maximum in λ_{100} is dependent on thermal history. In this investigation, we have used magnetic force microscopy (MFM) to characterize the domain morphologies of Fe–*x* at. % Ga for *x*=12, 20, and 25. Studies have been performed for crystals in both the as-received FC and post-annealed (PA) conditions.

II. EXPERIMENTAL PROCEDURE

Crystals used in this investigation were grown at Ames Laboratory by a Bridgman method as previously described.[9] The crystals were annealed at 1000 °C for 168 h, with heating and cooling rates of 10°/min, after which the crystals were considered to be in the FC state. All crystals were of

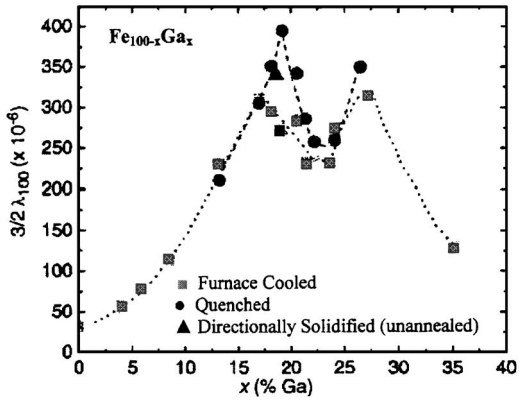

FIG. 1. $(3/2)\lambda_{100}$ as a function of Ga concentration for $Fe_{100-x}Ga_x$ (Ref. 7).

[a]Electronic mail: fbai@vt.edu

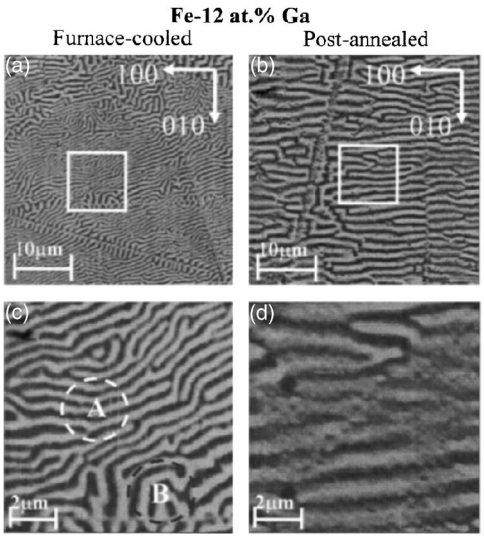

FIG. 2. MFM images of the (001) surface of Fe–12 at. % Ga at furnace-cooled condition, (a) and (c), and after being post annealed, (b) and (d). Region A shows an area populated by domains preferentially aligning along the [100] direction and region B shows broken domains and magnetic closure patterns.

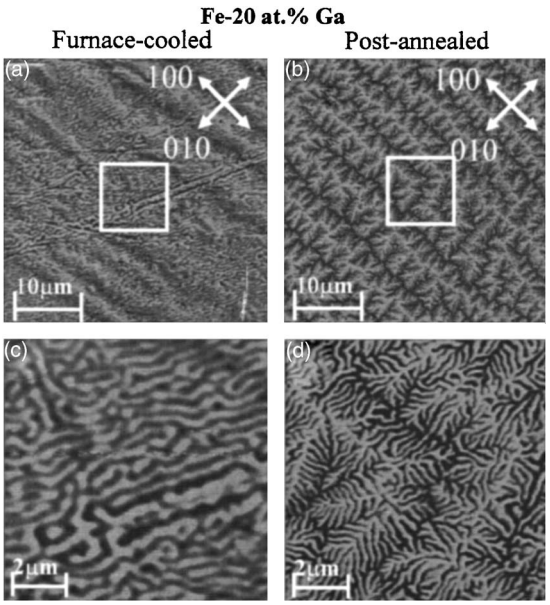

FIG. 3. MFM images of the (001) surface of Fe–20 at. % Ga at furnace-cooled condition, (a) and (c), and after being post annealed, (b) and (d).

dimensions $10\times10\times2$ mm^3. The (001)-oriented 10×10-mm^2 faces were polished down to 0.25-μm finish. Careful investigations were performed using MFM by starting from the FC state and then again after being PA at 700 °C or higher for 1 h. For each sample on different conditions, more than two spots were observed to obtain a representative domain structure. Magnetic force microscopy was carried out using a Vecoo DI 3100a scanning probe microscope (SPM) employing silicon cantilevers with tips coated with a CoCr film. All domain studies were carried out at ambient temperature, with the tip magnetized normally to the specimen surface. Topography images were obtained in the tapping mode and the magnetic force gradient images were obtained by phase scanning in the "interleave" mode using a typical lift height of 20 nm.

III. RESULTS

A. MFM images

Figures 2(a) and 2(c) show the domain structures of FC Fe–12 at. % Ga. To better illustrate the overall domain morphology and local domain features, images with different scan scales are shown. It should be noted that there are some magnetic defect lines on the MFM images due to physical scratches, however, these scratches are homogeneous in topography (not show here) and thus have little influence on our domain alignment analysis. In the region designated by the symbol A in part (c) of this figure, the magnetic domains can be seen on average to be aligned along the [100] direction. The domain width is ~0.5 μm and its length is $\geqslant10$ μm. However, we did find regions in which the domain alignment was disrupted, and a typical magnetic closure pattern was established, as designated by the symbol B. Domain structures of Fe–12 at. % Ga in the PA condition are shown in Figs. 2(b) and 2(d); again images with different scan scales are shown. A similar domain structure was found, except that the domains were much wider and also had a higher degree of [100] alignment. These slight differences in domain structures between the FC and PA conditions may reflect corresponding variations in the magnetostriction with thermal history that was previously reported.[7]

Figures 3 shows MFM images of the domain structure of Fe–20 at. % Ga. Parts (a) and (c) show the domain structure in the FC state. In part (a), small domains of micron size or below can be seen to be arranged within [001]-oriented domain platelets of 5–10-μm width and 30–50-μm length. Part (c) shows an image with a higher resolution of 10×10 μm^2 which better illustrates the features of the finer domains. These domains can be seen to be much smaller in size and much less regular than the corresponding ones for Fe–12 at. % Ga, as can be seen by comparing Figs. 2(c) and 3(c). The fine scale domains of FC Fe–20 at. % Ga were ~0.4 μm in width and <2 μm in length. These fine scale domains, or subdomains, tend to have some [010] preferential orientation; however, (i) the domain walls were often bent or rough, (ii) there was considerable bending between [010] and [100] variants, and (iii) there were domain regions not restricted to this crystallographic direction. Parts (b) and (d) show the domain structure in the PA state. The image in part (b) shows the presence of [001]-oriented domain platelets of 5–10-μm width and 30–50-μm length that have a finer internal domain structure—in these two regards, the results from the FC and PA conditions are similar. However, there was a significant difference between these two conditions with regards to the morphology and distribution of the fine domain structure within the platelets. Part (d) shows a higher-resolution image taken from an area of 10 μm^2. This image illustrates that the subdomains organize into dendrite morphology.

The appearance of subdomains with a dendritic morphology is indicative of a phase change, possibly to the DO3 structure as previously reported.[8] We confirmed this possibil-

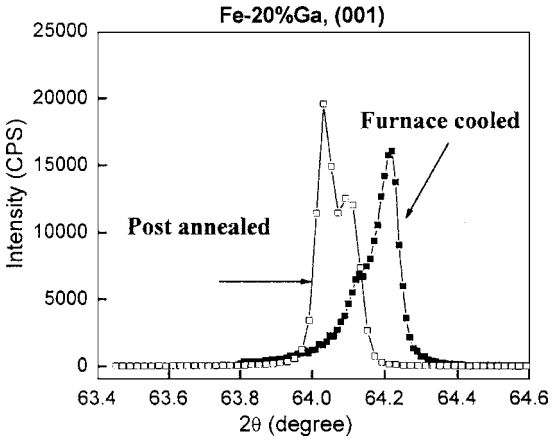

FIG. 4. (200) line scan of Fe–20 at. % Ga by XRD in the furnace-cooled condition and after being post annealed.

ity by x-ray diffraction (XRD), as shown in Fig. 4. A much stronger DO3 peak (left one) was observed in the PA state, relative to the FC state, and after post annealing, the lattice parameter also shifted to a higher value. Dendrite formation is indicative of a phase transformation by nucleation and growth, which is often rate limited by diffusion. This may provide important insight into the origin of the drop in magnetostriction upon annealing (see Fig. 1). Quenching prevents diffusion, favoring the disordered bcc structure of this phase; whereas annealing allows for diffusion and favors development of the ordered DO3 structure.

We also performed MFM studies for crystals with higher Ga contents. Figures 5(a) and 5(b) show the domain structures of Fe–25 at. % Ga in the FC and PA conditions, respectively. Similar domain structures were found for both conditions. Macrodomain platelets were not found, rather the only observable feature in the MFM images was the finer subdomains. The typical length and width of these subdomains are <1 μm and <0.2 μm, respectively. The fine domains have somewhat preferred alignment along the [010] direction, but notably less than that for lower Ga-content crystals. These results indicate that the DO3 phase is fully formed for Fe–25 at. % Ga. This was confirmed by XRD and is consistent with prior results which have reported the boundary between the two-phase (A2+DO3) and DO3 phase fields at about $x=23$ at. % Ga.[8]

B. Fast Fourier transformations of MFM images

Next, we performed fast Fourier transformations (FFTs) on the MFM images. This allowed us to obtain a better measure of domain alignment and features in both x and y directions. The FFT algorithm separates the original wave form into its constituent parts, mapping each wavelength on a two-dimensional (2D) spectral plot, providing information on (i) domain alignment—well-aligned domains have narrow frequency bands and thus sharp contrast in FFT images, (ii) domain orientation—the symmetry of the wavelength distribution reflects domain orientation, and (iii) the value of the wavelength represents the average width of aligned domains—the shorter wavelengths lie around the periphery of the plot, whereas the longer wavelengths lie near its center, and the center-most point is labeled as "dc" (for "direct current"), which corresponds to a size equal to that of the image.

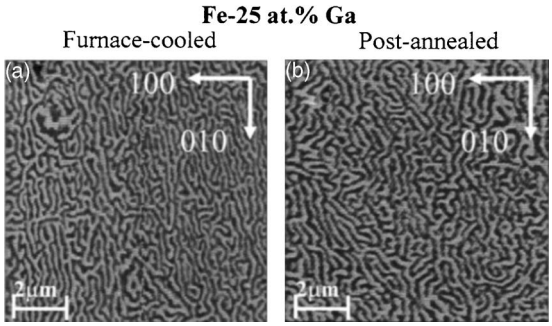

FIG. 5. MFM images of the (001) surface of Fe–25 at. % Ga in the furnace-cooled state (a) and after being post annealed (b) to show similar domain structures less preferentially aligned along [010].

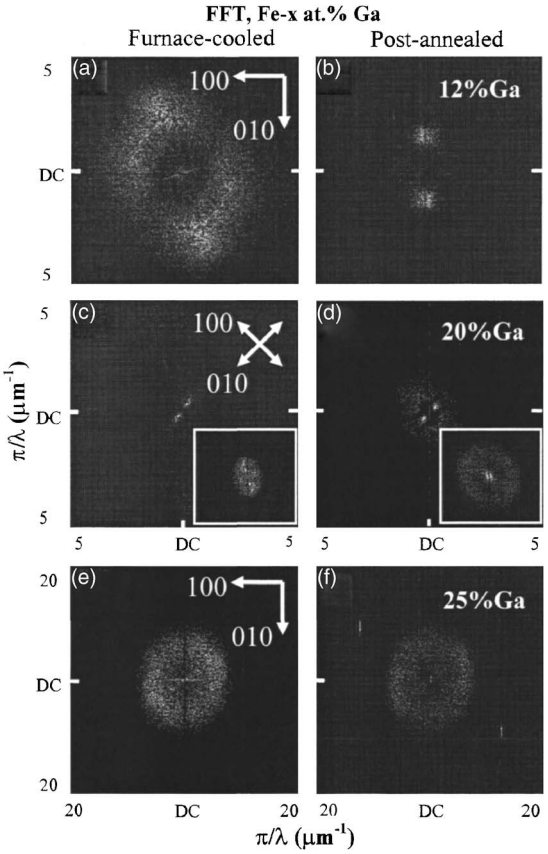

FIG. 6. FFT images of the (001) surface of Fe–12 at. % Ga, (a) and (b); Fe–20 at. % Ga, (c) and (d); and Fe–25 at. % Ga in the furnace-cooled and post-annealed state, (e) and (f), respectively. The insets are the FFT images corresponding to Figs. 3(c) and 3(d) with fine domain structure to show domain hierarchy in different scales. Both of the insets have a frequency scale from 20 μm^{-1} to dc.

Figures 6(a) and 6(b) show the FFT of the Fe–12 at. % Ga images originally given in Figs. 2(a) and 2(b), which are FC and PA states, respectively. A twofold symmetry along the x axis ([100] direction) can be seen for both images, clearly revealing that the domain structure has a significant degree of [100] preferred alignment, i.e., 180° oriented along [100]. In the FC condition, relative to the PA, we noticed (i) two additional peaks with notably weaker intensities that were slightly rotated away from the [010], indicating 90° domains that are slightly tilted presumably to relax the elastic energy, and (ii) that the intensity had a diffuse halo, with a relatively broad distribution of radii, indicating significant

domain size nonuniformity. The wavelengths were then determined to be $1.7<\lambda_x<4$ μm and $0.6<\lambda_y<0.9$ μm for the FC state, and λ_x=dc and $\lambda_y \approx 1.4$ μm for the PA state. These results clearly show that post annealing increases the domain size and its regularity.

Figures 6(c) and 6(d) show the FFT result of Fe–20 at. % Ga in the FC and PA states, originally shown in Figs. 3(a) and 3(b), respectively. Similar to 12 at. % Ga, a twofold symmetry was also found for Fe–20 at. % Ga, which was strictly aligned along [010]. The average wavelengths were $\lambda_x \approx 10$ μm and $\lambda_y \approx 10$ μm for the FC state, and $\lambda_x \approx 8$ μm and $\lambda_y \approx 8$ μm for the PA one—which corresponds to the size of the [100] macrodomain plates in the MFM image. We then obtained the FFT of the higher-resolution MFM images for Fe–20 at. % Ga [Figs. 3(c) and 3(d)], shown in the insets of Figs. 6(c) and 6(d), respectively. These insets show a diffuse halo with peaks close to the [100] and [010] directions. Post annealing was found to result in an increase in the diffuseness of the halo and an increase in its radii. The FFT of Fe–20 at. % Ga evidences hierarchal domains organized over different length scales, whose degree of organization and wavelengths are both decreased by post annealing.

Finally, Figs. 6(e) and 6(f) show FFTs of Fe–25 at. % Ga in the FC and PA states, respectively. (Please note the different frequency scales.) The signature feature of the FFT for Fe–25 at. % Ga crystals was a broad and diffuse halo, with $0.3<\lambda_R<0.5$ μm ($\lambda_R=\sqrt{\lambda_x^2+\lambda_y^2}$). The results indicate a lack of organization of the miniature domains into a crystallographically regular pattern, although weak intensity peaks indicate some residual domain alignment along [010].

IV. DISCUSSION AND SUMMARY

The results of our investigation demonstrate with increasing x that (i) the typical domain size is decreased, (ii) the domain morphology becomes increasingly irregular, and (iii) the degree of the [100] preferential orientation is reduced. These results clearly show increasing domain inhomogeneity with increasing Ga content. The enhancement of λ_{100} with increasing x below 19 (see Fig. 1) has previously been attributed to the emergence of directional short-range ordering of Ga atoms (i.e., Ga pairs).[10] However, our MFM results indicate that domain nonuniformity may also play a key role in enhanced magnetostriction. This may be due to an increase in the ease of domain movement—it is much easier to move a diffuse wall than a sharp one in the presence of quenched disorder.[11] Recent investigations by Wuttig *et al.*[12] and Clark *et al.*[7] have shown that the value of $1/2(C_{11}\text{-}C_{12})$ decreases as the Ga content is increased in the Fe–x at. % Ga solution. The combination of these prior results[7,12] and our present results indicate that metastable premartensitic states may be trapped by quenched disorder, as predicted by earlier theories of Kartha *et al.*[13]

The fact that the magnetic domains in Fe–12 at. % Ga had a strong degree of preferred [100] orientation on the (001) plane, instead of [100] and [010] closure domains, indicates an intrinsic deviation from a conventional bcc structure in the A2 phase. This crystallographic restriction is not unique to tetragonal structures, but rather can also be found in lower-symmetry orthorhombic and monoclinic domain variants, which have inequivalent c and a axes. Previous XRD studies of quenched Fe–19 at. % Ga crystals have shown that (i) the c axis of the tetragonal distortion lies parallel to the direction of Ga pairing[14] and (ii) an elongation of the diffraction peak (i.e., peak broadening) along the [101] direction in mesh scans, indicative of orthorhombic or lower-symmetry structural modulations.[15] These prior XRD results that indicate distortions from a conventional tetragonal domain variant are consistent with our observation of decreasing domain regularity with increasing x. It implies a heterophase region over a relatively large phase field, where the characteristic length scale of the DO3 phase depends on Ga content and thermal history.

In summary, the domain structure of furnace-cooled and post-annealed Fe–x at. % Ga crystals have been investigated by magnetic force microscopy for $12<x<25$. Our results indicate the importance of quenched disorder on a domain hierarchy. With increasing x, we have observed a decrease in (i) the typical size of the magnetic domains within macrodomain platelets, and a disappearance of the platelets in the DO3 phase field, (ii) the degree of domain regularity, and (iii) the degree of the [100] preferred orientation. Our results indicate enhanced magnetostriction for crystals with miniaturized domains that retain good [100] preferred orientation.

ACKNOWLEDGMENTS

We would like to gratefully acknowledge the Office of Naval Research under Grant Nos. N000140210340, N000140210126, and MURI N0000140110761. Two of the authors (D.W. and T.A.L.) acknowledge support of the U.S. Department of Energy, Office of Basic Energy Science, under Contract No. W-7405-ENG-82.

[1] *Handbook of Giant Magnetostrictive Materials*, edited by G. Engdahl (Academic, San Diego, 2000).
[2] A. E. Clark, M. Wun-Fogle, J. B. Restorff, T. A. Lograsso, A. R. Ross, and D. L. Schlagel, Proceedings of Actuator 2000 Conference, Berlin, Germany (unpublished).
[3] R. C. Hall, J. Appl. Phys. **30**, 816 (1960).
[4] Z. H. Liu *et al.*, Appl. Phys. Lett. **85**, 1751 (2004).
[5] G. D. Liu *et al.*, Appl. Phys. Lett. **84**, 2124 (2004).
[6] S. Guruswamy, N. Srisukhumbowornchai, A. E. Clark, J. B. Restorff, and M. Wun-Fogle, Scr. Mater. **43**, 239 (2000).
[7] A. E. Clark, K. B. Hathaway, M. Wun-Fogle, J. B. Restorff, T. A. Lograsso, V. M. Keppens, G. Petculescu, and R. A. Taylor, J. Appl. Phys. **93**, 8621 (2003).
[8] O. Ikeda, R. Kainuma, I. Ohnuma, K. Fukamichi, and K. Ishida, J. Alloys Compd. **347**, 198 (2002).
[9] A. E. Clark, M. Wun-Fogle, J. Restorff, and T. Lograsso, *Proceedings of the Fourth Pacific Rim International Conference on Advanced Materials and Processing (PRICM4)*, edited by S. Hanada, Z. Zhong, S. Nam, and R. Wright (The Japan Institute of Metals, 2001), p. 1711.
[10] J. R. Cullen, A. E. Clark, M. Wun-Fogle, J. B. Restorff, and T. A. Lograsso, J. Magn. Magn. Mater. **226**, 948 (2001).
[11] Y. Imry and S. Ma, Phys. Rev. Lett. **35**, 1399 (1975).
[12] M. Wuttig, L. Dai, and J. Cullen, Appl. Phys. Lett. **80**, 1135 (2002).
[13] S. Kartha, T. Castan, J. A. Krumhansl, and J. Sethna, Phys. Rev. Lett. **67**, 3630 (1991).
[14] T. A. Lograsso, A. R. Ross, D. L. Schlagel, A. E. Clark, and M. Wun-Fogle, J. Alloys Compd. **350**, 95 (2003).
[15] D. Viehland, J. F. Li, T. A. Lograsso, and M. Wuttig, Appl. Phys. Lett. **81**, 3185 (2002).